NJC

Accepted Manuscript

This is an *Accepted Manuscript*, which has been through the Royal Society of Chemistry peer review process and has been accepted for publication.

Accepted Manuscripts are published online shortly after acceptance, before technical editing, formatting and proof reading. Using this free service, authors can make their results available to the community, in citable form, before we publish the edited article. We will replace this *Accepted Manuscript* with the edited and formatted *Advance Article* as soon as it is available.

You can find more information about *Accepted Manuscripts* in the Information for Authors.

Please note that technical editing may introduce minor changes to the text and/or graphics, which may alter content. The journal's standard Terms & Conditions and the Ethical guidelines still apply. In no event shall the Royal Society of Chemistry be held responsible for any errors or omissions in this *Accepted Manuscript* or any consequences arising from the use of any information it contains.

ROYAL SOCIETY OF CHEMISTRY

www.rsc.org/njc

Electronic and Optical properties of 5-AVA Functionalized BN Nanoclusters: A DFT Study

Alireza Soltani[a,*], Ahmad Sousaraei[a], Masoud Bezi Javan[b], Mortaza Eskandari[c], Hanzaleh Balakheyli[d]

[a]Young Researchers and Elite Club, Gorgan Branch, Islamic Azad University, Gorgan, Iran

[b]Physics Department, Faculty of Sciences, Golestan University, Gorgan, Iran

[c]Department of Chemistry, Institute for Advanced Studies in Basic Sciences, Gavazang, Zanjan, Iran

[d]Joints, bones and connective tissue research center, Golestan University of Medical Science, Gorgan, Iran

* Corresponding author. E-mail: Alireza.soltani46@yahoo.com, g.chem1983@gmail.com, Tel: +98-938-4544921

Abstract

We have carried out detailed density functional theory (DFT) and Time-dependent density functional theory (TD-DFT) calculations upon 5-aminolevulinic acid-functionalized $B_{12}N_{12}$ and $B_{16}N_{16}$ nanoclusters at the B3LYP, B3PW91, and PBE methods with 6-311+G** basis set. The calculated adsorption energies of the 5-aminolevulinic acid with the BN nanoclusters evaluated at T = 298.15 and 311.15 K in the gaseous and aqueous environments at the B3LYP, B3PW91, and PBE methods. Our results exhibited that the adsorption of 5-AVA molecule (NH_2 group) with $B_{12}N_{12}$ is more favorable than in $B_{16}N_{16}$ nanocluster in the gas and solvent phases. It is anticipated that 5-aminolevulinic acid (5-AVA) drug incorporating BN clusters will be extended as drug delivery systems and biomedical devices.

Keywords: BN nanoclusters, 5-aminolevulinic acid, Adsorption, Nonliner optical, Electronic structure

1. Introduction

Bioconjugated nanostructure materials have become visible as novel materials for medical diagnostics and biosensing applications in recent years.[1,2] Pristine BN nanostructures are known as promising candidates for this means. Boron nitride nanotubes (BNNTs), a morphologically similar prototype of carbon nanotubes (CNTs) with different properties of their own, with the abilities of uniformity and stability in dispersion in solution are known as promising candidates for biomedical applications.[3-6] Their electronic structures and properties widely vary owing to tube helicity and concentric layers, unlike CNTs and their semiconducting property, regardless of their diameter and chirality that make these materials suitable for electronic applications.[7,8] The BNNTs are renowned as nontoxic materials to health and environment owing to their chemical inertness and structural stability, and hence, they are useful in the development of drug delivery, novel biosensors, biofunctional materials, nanovectors for cell therapy, drug, and gene delivery studies.[9-13] Within the hemechromophore in mitochondria a compound called 5-Aminolevulinic acid (5ALA) is considered as a key synthetic building block in protoporphyrin IX (PpIX). Under a negative feedback control mechanism of heme, ALA could be synthesized in mitochondria. Basically, the mechanism is initiated by the building of glycine and succinyl CoA, being catalyzed via ALA-syntase, making the first intermediate synthesizing agent that undergoes a series of biochemical reactions. Consequently, in the presence of iron, the PpIX is converted into heme by ferrochelatase. A great deal of attention has been paid upon the inclination of 5-ALA for inducing protoporphyrin IX (PpIX) in tumor cells after its exogenous administration. It was used to detect or photo destruction of malignant tissue and in the preoperative delineation of malignant brain tumors due to its fluorescence and photosensitizing properties that resulted to lengthen the patient survival.[14,15] The recent strategies in PDT (Photodynamic therapy) for the patients include prescribing the extra amount of 5-ALA and or alkyl esters. Through three

approaches; direct injection into the tissue, administration of the blood, or by topical application to the skin.[16,17] Recently, a broad variety of investigations has been performed upon the electrical and structural properties of pure and functionalized 5-ALA, Eriksson and Erdtman have carried out a theoretical study of 5-Aminolevulinic acid and some pharmaceutically important derivatives.[14] Ganji et al. Have done a DFT study upon the interaction of $B_{36}N_{36}$ cluster with glycine amino acid.[18] Gou and co-workers[19] performed DFT calculations to investigate non-covalent functionalization of BN nanotubes with perylene derivative molecules. Xie et al. experimentally found that BN nanotube can be functionalized with amino-based systems. Regarding noncovalent functionalizations of BNNTs by aromatic compounds, surfactants, and polymers, via π–π stacking interaction has drawn growing attention due to their potential applications in upgrading the novel biosensors, biofunctional materials, nanovectors for cell therapy, drug, and gene delivery.[20] Zhao and Ding used theoretical calculations to investigate the interaction of non-covalent functionalization of BN nanotubes by various aromatic molecules.[21] Zhi et al. has studied that BN nanotubes can be noncovalently functionalized by wrapping them with DNA.[22] Very recently, Ciofani et al. experimentally investigated that the BN nanotubes can be coated by polyethyleneimine (PEI), indicating the essential stipulations for the biomedical applications of BN nanotubes.[12] In previous theoretical work,[23] we performed the interaction of 5-ALA drug with carbon nanostructures using DFT calculations. Herein, we aim to consider the electronic and structural properties of the 5-ALA functioned with $B_{12}N_{12}$ and $B_{16}N_{16}$ nanoclusters to further understanding of $B_{12}N_{12}$ and $B_{16}N_{16}$ capacity for drug delivery applications.

2. Computational Methods

Geometry optimizations, density of states (DOS), frontier molecular orbital (FMO), and natural bond orbital (NBO) analyses were performed with the GAMESS quantum chemistry software package.[24] All calculations are based on the density functional theory (DFT) and Time-dependent density functional theory (TD-DFT) at the B3LYP method with the standard 6-311+G** basis set.[25] The B3LYP is indicated to be a dependable and usually applied functional in the study of different BN nanostructures.[26-28] We have performed the exchange-correlation functional parameterized by PBE and B3PW91 with superposition error (BSSE) correction.[29,30] In the PCM calculations, water was used as a solvent, through the value ε = 78.4 of the dielectric constant. Adsorption calculations were carried out in gaseous and aqueous environments, at T = 298.15 and 310.15 K. After optimization, the obtained B-N bond length of $B_{12}N_{12}$ is about 1.486, 1.493, and 1.492 Å and are 1.473, 1.481, and 1.480 Å in 4-cycle for $B_{16}N_{16}$ cage at the B3LYP, PBE, and B3PW91 methods, respectively (see Table 1). The adsorption energies (E_{ad}) of 5-AVA upon the pure BN nano-cages are represented by:

$$E_{ad} = E_{cage\text{-}Molecule} - (E_{cage} + E_{Molecule}) + E_{BSSE} \quad (1)$$

where E_{cage} is the adsorption energies of the pristine $B_{12}N_{12}$ and $B_{16}N_{16}$ nano-cages. $E_{cage\text{-}Molecule}$ is the adsorption energy of 5-AVA interacting with the pristine $B_{12}N_{12}$ and $B_{16}N_{16}$ clusters and $E_{Molecule}$ represents the energy of an isolated 5-AVA molecule. The quantum molecular descriptors [31,32] for nano-cage were determined as follows:

$$\mu = -(I + A)/2 \quad (2)$$

$$\chi = -\mu \quad (3)$$

$$\eta = (I - A)/2 \quad (4)$$

$$S = 1/2\eta \quad (5)$$

$$\omega = (\mu^2/2\,\eta) \quad (6)$$

The electronegativity (χ) is defined as the negative of chemical potential (μ), as follows: $\chi = -\mu$. Furthermore, the global hardness (η) can be determined using the Koopmans' theorem. I ($-E_{HOMO}$) is the ionization potential and A ($-E_{LUMO}$) is the electron affinity of the molecule.

Table 1 Calculated the structural and electronic properties of $B_{12}N_{12}$ and $B_{16}N_{16}$ nano-cages at the B3PW91, B3LYP, and PBE methods.

	B3LYP		B3PW91		PBE	
system	$B_{12}N_{12}$	$B_{16}N_{16}$	$B_{12}N_{12}$	$B_{16}N_{16}$	$B_{12}N_{12}$	$B_{16}N_{16}$
$R_{B\text{-}N}$/Å	1.486	1.473	1.485	1.471	1.494	1.481
$R_{B\text{-}N\text{-}B}$/°	80.50	78.53	80.12	78.15	79.95	77.85
$R_{N\text{-}B\text{-}N}$/°	98.23	99.34	98.44	99.56	98.58	99.81
$R_{N\text{-}B\text{-}N}$/°						
Q_B/e	0.450	0.44	0.459	0.482	0.387	0.389
Q_N/e	-0.450	-0.44	-0.459	-0.482	-0.387	-0.390
E_{HOMO}/eV	-7.85	-7.38	-7.98	-7.56	-6.91	-6.49
E_{LUMO}/eV	-1.11	-1.01	-1.05	-1.10	-1.92	-1.88
E_g/eV	6.74	6.37	6.93	6.46	4.99	4.61
E_{FL}/eV	-4.48	-4.20	-4.52	-4.33	-4.42	-4.19
μ/eV	-4.48	-4.19	-4.52	-4.33	-4.42	-4.19
η/eV	3.37	3.19	3.47	3.23	2.50	2.31
ω/eV	2.98	2.76	2.94	2.90	3.91	3.80
S/eV	0.15	0.16	0.14	0.15	0.20	0.22
χ/eV	4.48	4.19	4.52	4.33	4.42	4.19
D_M/Debye	0.00	0.0	0.0	0.0	0.0	0.0

3. Results and discussion

Initially, we computionally optimized the geometry of individual 5-Aminolevulinic acid molecule (5-AVA) within the gas phase; see Fig. 1 and Table 2. It exhibits the optimized geometry of the individual 5-Aminolevulinic acid molecule. All the nitrogen and oxygen atoms form essentially a planar structure with carbon atoms implying sp^2 orbital hybridization, maintaining the aromatic characteristics. Fig. 1**a-c** indicates the molecular electrostatic potential (MEP), the highest occupied molecular orbital (HOMO), and the lowest unoccupied molecular orbital (LUMO) of a 5-Aminolevulinic acid molecule. It is apparent that the electron densities in the HOMO and LUMO are situated upon the amine and carbonyl orbitals of the molecule and is upon the CH_2 group. The energy gap (E_g) and Fermi level (E_F) of the 5-Aminolevulinic acid molecule are 2.21 and -3.57 eV at B3LYP method, respectively. This result reveals that the 5-Aminolevulinic acid molecule with a large energy gap is hard molecule.[31] Also, the dipole moment (D_M) of this drug molecule is about 2.27 Debye. The relaxed geometries of 5-AVA-$B_{12}N_{12}$ and 5-AVA-$B_{16}N_{16}$ systems at the B3LYP method are shown in Figs. 2**A-C** and 3**A-C**. To evaluate the preferred interaction, the interaction of 5-AVA drug upon the boron atoms of $B_{12}N_{12}$ and $B_{16}N_{16}$ clusters was studied. The chemisorption energy of 5-AVA molecule from its $-NH_2$ group close to $B_{12}N_{12}$ and $B_{16}N_{16}$ clusters are calculated to be -1.33 and -1.20 eV, respectively (see Table 3). The distance of drug molecule with the NH_2 group attached to the B atoms of $B_{12}N_{12}$ and $B_{16}N_{16}$ nanoclusters are 1.629 and 1.638 Å, respectively. NBO reveals that notable charge transfers are occurred of 0.337 and 0.274 electrons from 5-AVA molecule to $B_{12}N_{12}$ and $B_{16}N_{16}$ nanoclusters as a donor. We noted that the interaction of 5-AVA drug upon the $B_{12}N_{12}$ cluster has the largest adsorption energy, while the interaction of this drug molecule with $B_{16}N_{16}$ nanocluster is the smallest (see Fig 3**A-C**).

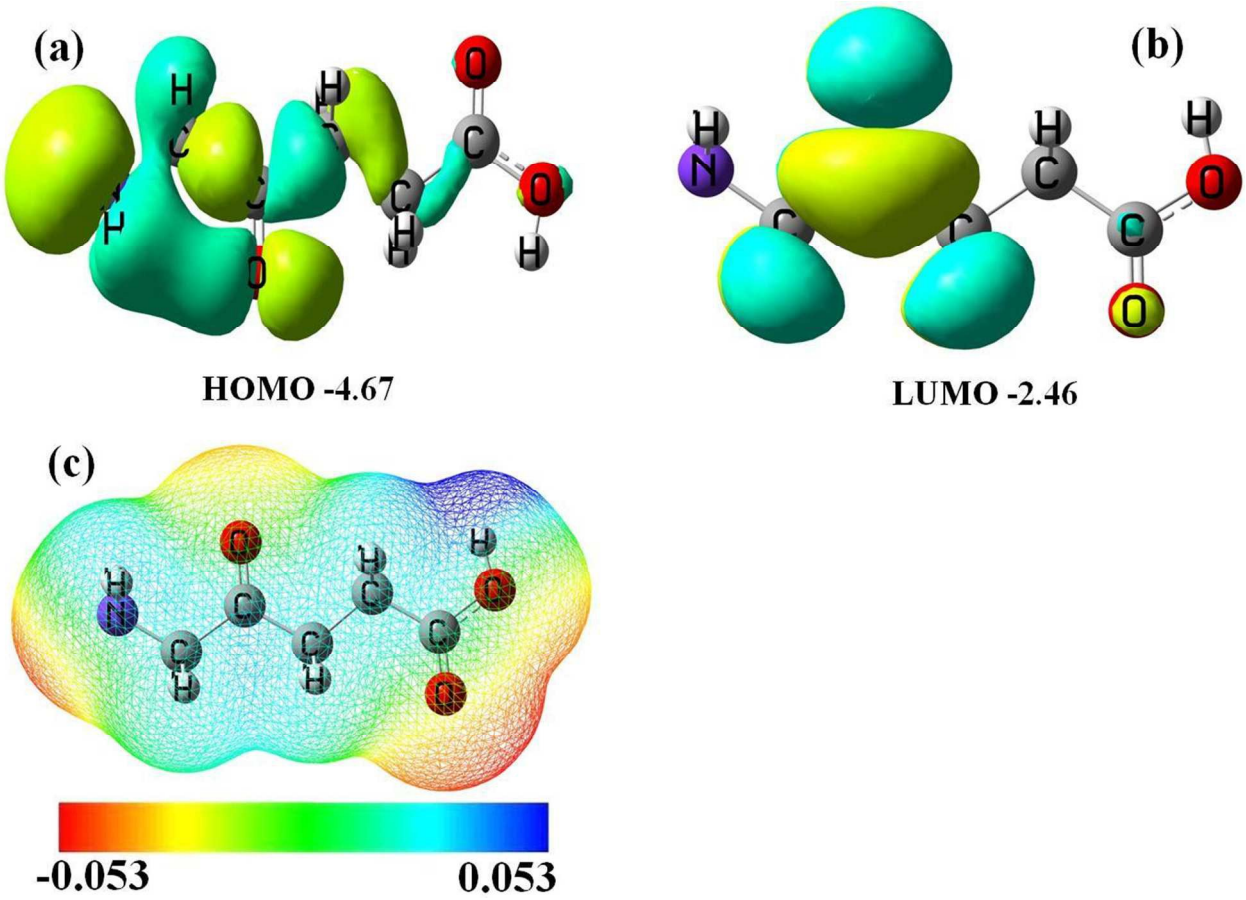

Fig. 1. The profiles of HOMO (**a**), LUMO (**b**), and MEP (**c**) of 5-aminolevulinic acid at the B3LYP method.

Table 2 Results obtained from geometry optimizations of 5-aminolevulinic acid molecule at the B3LYP method.

System	R_{C-N}/Å	R_{C-H}/Å	R_{C-O}/Å	R_{O-H}/Å	R_{C-C-C}/°	R_{C-C-N}/°	$R_{N-C-C-C}$/°	$R_{C-C-C-C}$/°
R_{B-N}/Å	1.452	1.095	1.212	0.964	116.6	116.1	179.6	179.5

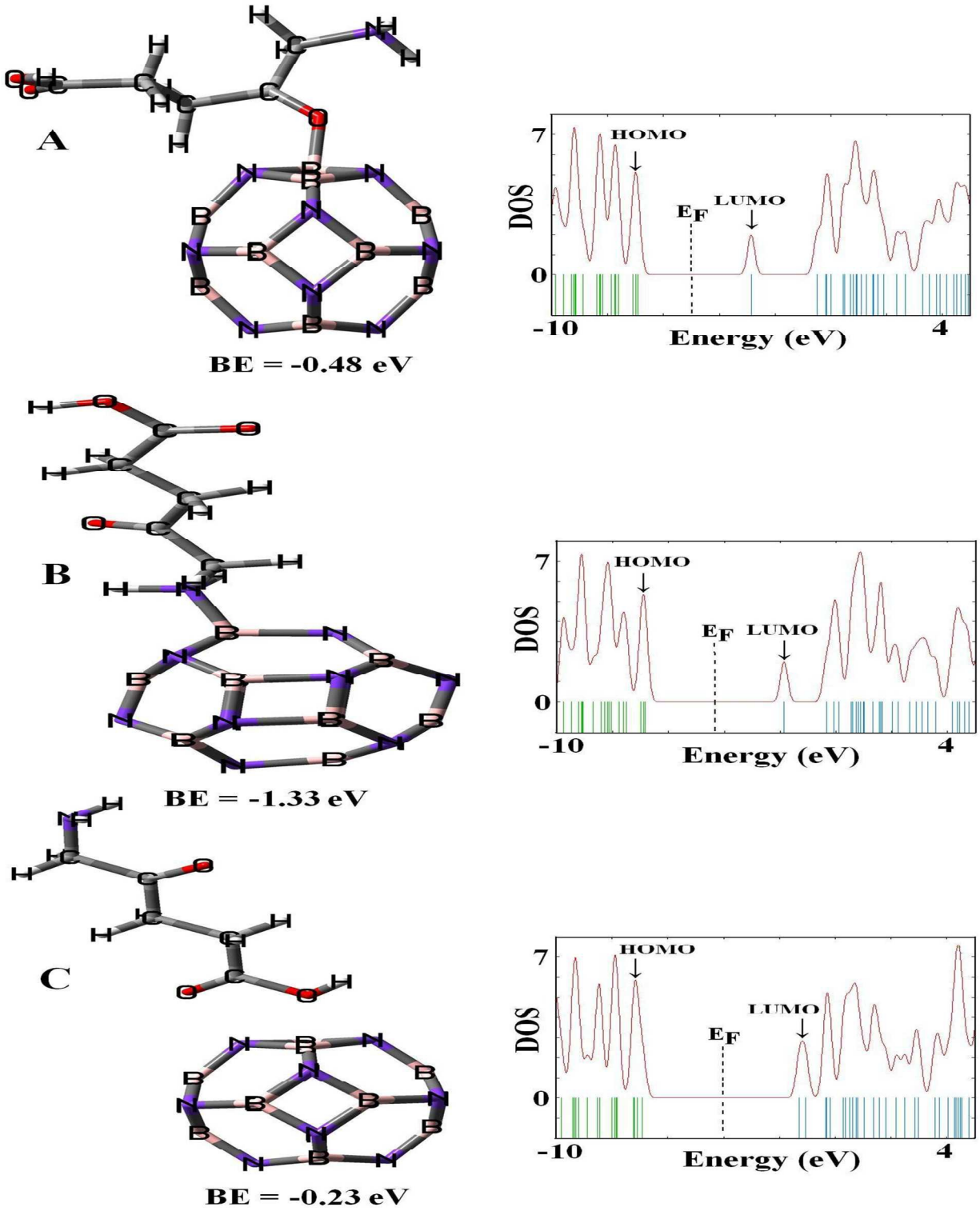

Fig. 2. Optimized structures and the electronic density of states of 5-aminolevulinic acid over $B_{12}N_{12}$ nano-cage.

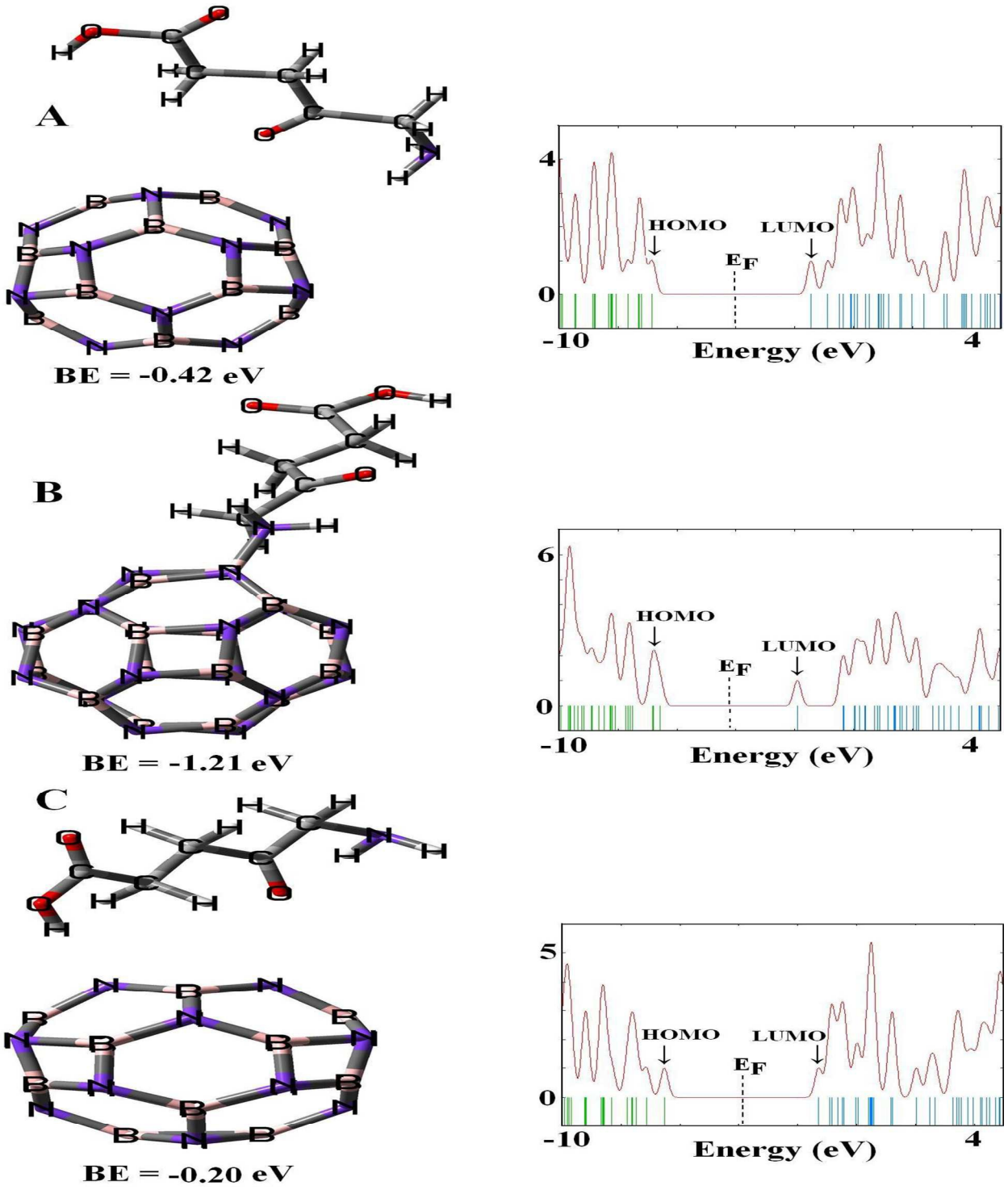

Fig. 3. Optimized structures and the electronic density of states of 5-aminolevulinic acid over $B_{16}N_{16}$ nano-cage.

Table 3 Calculated the structural and electronic properties of 5-aminolevulinic acid molecule interacted with $B_{12}N_{12}$ and $B_{16}N_{16}$ nano-cages at the B3LYP method.

system	$NH_2/B_{12}N_{12}$	$CO/B_{12}N_{12}$	$OH/B_{12}N_{12}$	$NH_2/B_{16}N_{16}$	$CO/B_{16}N_{16}$	$OH/B_{16}N_{16}$
R_{B-N}/Å	1.515	1.548	1.539	1.553	1.488	1.486
R_{B-N-B}/°	83.80	84.35	82.45	82.13	79.34	78.10
R_{N-B-N}/°	92.15	92.40	94.29	93.15	98.20	99.12
R_{N-B-N}/°						
R_{NH2}/ Å	1.023	1.018	1.019	1.023	1.019	1.020
R_{CO}/ Å	1.218	1.244	1.218	1.218	1.224	1.220
R_{OH}/ Å	0.972	0.972	0.980	0.972	0.972	0.981
D/Å	1.629	1.616	1.822	1.638	2.310	2.016
E_{ad}/eV	-1.33	-0.48	-0.23	-1.20	-0.42	-0.20
Q_B/e	0.628	0.621	0.601	0.652	0.558	0.499
Q_N/e	-0.515	-0.545	-0.524	-0.510	-0.491	-0.552
$Q_{NH2\text{-}AVA}$/e	-0.693	-0.681	-0.682	-0.710	-0.704	-0.684
$Q_{CO\text{-}AVA}$/e	-0.446	-0.387	-0.394	-0.446	-0.433	-0.457
$Q_{OH\text{-}AVA}$/e	-0.561	-0.557	-0.610	-0.561	-0.567	-0.614
E_{HOMO}/eV	-6.84	-6.93	-6.91	-6.59	-6.85	-6.53
E_{LUMO}/eV	-1.86	-2.86	-1.28	-1.91	-1.44	-1.29
E_g/eV	4.98	4.07	5.63	4.68	5.41	5.24
ΔE_g (%)	-27.20	40.58	-17.69	-26.5	-20.91	-23.39
E_{FL}/eV	-4.35	-4.90	-4.10	-4.25	-4.15	-3.91
μ/eV	-4.35	-4.90	-4.10	-4.25	-4.15	3.91
η/eV	2.49	2.04	2.82	2.34	2.71	2.62
ω/eV	3.80	5.89	2.98	3.86	3.18	2.92
S/eV	0.20	0.25	0.18	0.21	0.18	0.19
χ/eV	4.35	4.90	4.10	4.25	4.15	3.91

D_M/Debye	7.67	6.57	5.66	7.40	1.197	3.99

Then, we compared the present studies with the adsorption of 5-AVA molecule to the pristine carbon nanostructures of the previous reports.[23] The calculated binding energy of 5-AVA molecule in active sites, including NH_2 and CO groups interacting with C_{24} nano-cage is about -0.79 and -0.89 eV, at the B3LYP method, respectively. Based on this research, the interaction energy of 5-AVA molecule with the carbon nano-cage is significantly unstable by its active sites in comparison with that of the BN nano-cages. Based on the acquired results, the B-N bond length and N-B-N angle of 5-AVA/ $B_{12}N_{12}$ complex were found to be 1.564 Å and 92.15˚, while for 5-AVA/$B_{16}N_{16}$ complex are 1.569 Å and 93.15˚, respectively. Upon the interaction processes, the N-H bond length and H-N-H angle of the 5-AVA molecule are 1.024 Å and 105.02˚, respectively. The bond lengths of C-N and C-O in the pure 5-AVA molecule is 1.453 and 1.219 Å at the B3LYP method, respectively. Erdtman and Eriksson [14] have shown that the C-N and C-O lengths of 5-AVA molecule are about 1.457 and 1.226 Å at the B3LYP/6-31+G* level, respectively, which is comparable with our results. Calculated binding energies of 5-AVA molecule from its -OH group with the two systems, including $B_{12}N_{12}$ and $B_{16}N_{16}$ nanoclusters, having binding energies of -0.23 and -0.20 eV with the distances of 1.82 and 2.01 Å, respectively. Anota and Cocoletzi [33] have shown the adsorption between the metformin molecule and (5, 5) BNNT with the energy value of -0.63 eV, which is a result of exothermic process. We also calculated the adsorption of 5-AVA molecule in the most stable configuration (from its NH_2 group) towards $B_{12}N_{12}$ and $B_{16}N_{16}$ clusters at the PBE functional (see Table 4). The binding energies acquired for the 5-AVA molecule (NH_2 group) upon the B atoms of $B_{12}N_{12}$ and $B_{16}N_{16}$ clusters are includes with the exothermic adsorption energies of -1.49 and -1.38 eV, respectively. They are very different from the above theoretical values (B3LYP method). The smaller atomic

distances between the N atom of a molecule and the B atoms of $B_{12}N_{12}$ and $B_{16}N_{16}$ clusters are 1.630 and 1.638 Å, respectively. Besides, the interaction of 5-AVA molecule with BN nanoclusters at the PBE method indicates a considerable reduction in adsorption energy compared with the B3LYP method. The N-H bond length in the 5-AVA molecule added to $B_{12}N_{12}$ and $B_{16}N_{16}$ clusters are 1.036 and 1.031 Å, respectively, larger than the isolated 5-AVA bond length (N-H= 1.023 Å). Whereas the B-N lengths of $B_{12}N_{12}$ and $B_{16}N_{16}$ clusters after the adsorption of 5-AVA molecule are found to be 1.576 and 1.554 Å, respectively. Therefore, we are believed that the covalent interaction at the above mentioned separation will be strong in nature. MPA reveals that notable charge transfers are occurring in 0.321 and 0.320 electrons from 5-AVA molecule to $B_{12}N_{12}$ and $B_{16}N_{16}$ clusters at the PBE functional. These results clearly show that the charge transfer occurred for both systems are almost the same. Ganji et al. introduced the binding energy of Glycine molecule adsorbed upon $B_{36}N_{36}$ cage with the energy value of -1.15 eV of the PBE method.[18] In contrast, when the 5-AVA molecule adsorbed upon $B_{12}N_{12}$ and $B_{16}N_{16}$ nanoclusters at the PBE method exhibits that the binding energies for both two systems are reduced with notable changes as compared with that from B3LYP method. The adsorption energies of isoniazid drug upon the (5, 5) and (10, 0) BN nanotubes have been reported with the values of -0.649 and -0.738 eV at the PBE functional, respectively.[34] The adsorption energy of the 5-AVA molecule is close to $B_{12}N_{12}$ nanocluster therefore its appears to be stronger than those in the 5-AVA molecule interacting with $B_{16}N_{16}$ nanocluster. When the 5-AVA molecule from its NH_2 group interaction with the B atoms of $B_{12}N_{12}$ and $B_{16}N_{16}$ clusters, the values of the electric dipole moment are significantly increased from 0.0 Debye in the pure structures in 7.67 and 7.40 Debye in the complexes at the PBE method, respectively. As it is calculated by the PBE method, the dipole moment values for 5-AVA approaching to $B_{12}N_{12}$ and

$B_{16}N_{16}$ nanoclusters have significantly increased from zero in the pure structures in 7.48 and 7.40 Debye in the complex configurations, respectively. In other words, we consider the interaction of 5-AVA with $B_{12}N_{12}$ and $B_{16}N_{16}$ nanoclusters with the contact values of 1.623 and 1.630 Å at the B3PW91 functional. It is found that the adsorption of 5-AVA molecule with $B_{12}N_{12}$ and $B_{16}N_{16}$ clusters is exothermic with the high negative values of -1.39 and -1.30 eV, respectively. The high negative E_{ad} of 5-AVA drug upon the exterior surfaces of $B_{12}N_{12}$ and $B_{16}N_{16}$ nanoclusters indicates the chemical nature of the interaction. NBO reveals that notable charge transfers are occurring in 0.304 and 0.299 electrons from 5-AVA molecule to $B_{12}N_{12}$ and $B_{16}N_{16}$ nanoclusters at the B3PW91 functional. In the adsorption process between the adsorbate and adsorbent a locally structural deformation is attributed to the change from sp^2 to sp^3 hybridization of the B atom, where the sidewall boron atom is significantly pulled out of the surface (about 0.1 Å), indicating that the interaction is mainly covalent in nature. The D_M for 5-AVA molecule close to $B_{12}N_{12}$ and $B_{16}N_{16}$ clusters are significantly increased to 7.48 and 7.34 Debye at the B3PW91 functional, respectively (Table 4).

Fig. 4 indicates HOMO (highest occupied molecular orbital) and LUMO (lowest unoccupied molecular orbital) profiles for 5-AVA molecule (NH_2 group) toward $B_{12}N_{12}$ nanocluster. These profiles represent that the HOMO orbital is mainly localized on the nano-cage and the LUMO orbital is localized on the drug molecule. As shown in Fig. 4, the LUMO+1, LUMO+2, and LUMO+3 are located at the higher energy levels compared to the LUMO while the HOMO-3 is located at the lower energy level compared to the HOMO. These profiles imply that the value of E_{ad} in HOMO-LUMO orbital interactions depends on the *overlap and energy match* between the mixing orbitals and a greater energy discrepancy between the interacting HOMO and LUMO leads to higher E_{ad}.

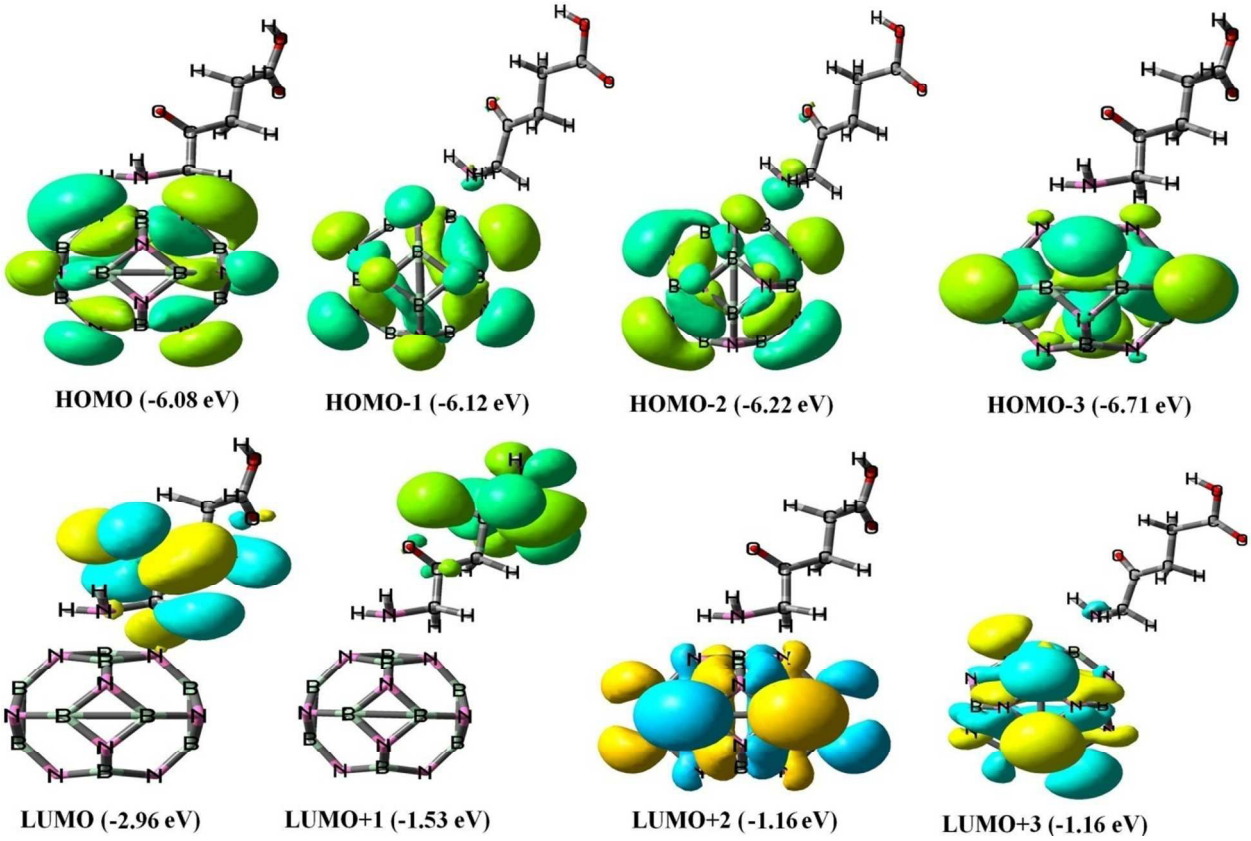

Fig. 4. Isosurfaces of HOMO and LUMO orbitals of 5-aminolevulinic acid over $B_{16}N_{16}$ nano-cage.

Table 4 Calculated the structural and electronic properties of 5-aminolevulinic acid molecule interacted with $B_{12}N_{12}$ and $B_{16}N_{16}$ nano-cages at the B3PW91 and PBE methods.

	B3PW91			PBE		
System	$NH_2/B_{12}N_{12}$	$CO/B_{12}N_{12}$	$OH/B_{12}N_{12}$	$NH_2/B_{12}N_{12}$	$CO/B_{12}N_{12}$	$OH/B_{12}N_{12}$
R_{B-N}/Å	1.566	1.545	1.541	1.576	1.575	1.552
R_{B-N-B}/°	83.37	84.17	82.89	83.39	84.20	82.15
R_{N-B-N}/°	92.24	92.58	94.20	92.29	92.57	94.32

R_{NH2}/Å	1.021	1.014	1.015	1.032	1.023	1.025
R_{CO}/Å	1.210	1.237	1.209	1.223	1.252	1.222
R_{OH}/Å	0.963	0.963	0.970	0.974	0.975	0.981
D/Å	1.617	1.613	1.775	1.630	1.622	1.797
E_{ad}/eV	-1.39	-0.51	-0.23	-1.49	-0.63	-0.32
Q_B /e	0.548	0.524	0.563	0.472	0.432	0.471
Q_N /e	-0.398	-0.430	-0.409	-0.347	-0.375	-0.361
$Q_{N\text{-}AVA}$ /e	-0.385	-0.439	-0.442	-0.362	-0.408	-0.414
$Q_{CO\text{-}AVA}$/e	-0.310	-0.237	-0.310	-0.271	-0.191	-0.265
$Q_{OH\text{-}AVA}$/e	-0.303	-0.299	-0.375	-0.263	-0.260	-0.321
E_{SOMO}/eV	-7.15	-7.22	-7.14	-6.08	-6.17	-5.91
E_{LUMO} /eV	-2.01	-2.98	-1.49	-2.96	-3.85	-2.42
E_g/eV	5.14	4.24	5.66	3.12	2.32	3.49
ΔE_g (%)	-25.83	-38.82	-18.33	-37.47	-53.51	-30.06
E_{FL}/eV	-4.58	-5.10	-4.32	-4.52	-5.01	-4.17
μ/eV	-4.58	-5.10	-4.32	-4.52	-5.01	-4.17
η/eV	2.57	2.12	2.83	1.56	1.16	1.75
ω/eV	4.08	6.13	3.30	6.55	10.82	4.97
S/eV	0.19	0.24	0.18	0.32	0.43	0.29
χ/eV	4.58	5.10	4.32	4.52	5.01	4.17
D_M/Debye	7.48	6.47	6.02	7.48	6.45	6.70

The adsorption behavior of 5-AVA molecule toward $B_{12}N_{12}$ nanocluster under different temperatures (from 298.15 to 311.15 K) at the gas phase was studied (Table 5). The results indicate that the adsorption energy initially decreases with increasing temperature. As a result, the highest adsorption energy can be observed at 298.15 K and the lowest minimum adsorption energy can be obtained at 398.15 K. The adsorption energies between the 5-AVA molecule and

$B_{12}N_{12}$ cluster at the temperature 398.15 K are calculated to be -1.37, -1.45, and -1.54 eV at the B3LYP, B3PW91, and PBE, respectively, suggesting that the adsorption behaviors of drug molecule are exothermic processes. The different energy distribution found in adsorption behavior at 398.15 K has no effect on the distance between the drug molecule and adsorbent (1.629, 1.623, and 1.631 Å at the B3LYP, B3PW91, and PBE, respectively). Solvation energies (E_{solv}) of the pure $B_{12}N_{12}$ interacted with the 5-AVA molecule has been studied at the B3LYP, B3PW91, and PBE methods of optimizing the structures in the vacuum and water compared to that in the gas phase (see Table 6). The difference between these optimization energies equals to E_{solv}. The solvation energies have been computed with the aid of the 'Conductor-like Screening Model' for solvation.[31] More negative E_{solv} will result in a higher degree of solubility. The solvation energy values of 5-AVA drug molecule are calculated to be -0.38, -0.39, and -0.34 eV at the B3LYP, B3PW91, and PBE methods, respectively. E_{solv} values for 5-AVA drug with $B_{12}N_{12}$ nano-cage is about -1.42, -1.51, and -1.59 eV at the B3LYP, B3PW91, and PBE methods, respectively. On loading 5-AVA drug molecule toward the $B_{12}N_{12}$ nano-cage, E_{solv} gets a further deduction showing an increase in the solubility of drug molecule in the presence of solvent. The molecular electrostatic potential (MEP) maps for 5-AVA molecule interacting with $B_{12}N_{12}$ and $B_{16}N_{16}$ clusters were studied (Fig. 5). MEP maps indicate that in the adsorption of drug molecule with clusters are positively charged (blue color with low intensity) while the N atoms are negatively charged (red color with high intensity) and the B atoms are positively charged (blue color) in the B-N bonds of the cluster, therefore, the drug molecule functions as an electron donor and the cluster functions as an electron acceptor owing to a strong adsorption. The semiconducting properties of $B_{12}N_{12}$ and $B_{16}N_{16}$ nanoclusters with energy gaps of about 6.74 and 6.37 eV, respectively, can be seen in the computed DOS plots from B3LYP method, as shown in

Fig. 3. Whereas the energy gaps of $B_{12}N_{12}$ and $B_{16}N_{16}$ clusters are calculated to 4.99 and 4.61 eV at the PBE method, respectively, with a value significantly smaller than the E_g in B3LYP method. The energy gap of $B_{12}N_{12}$ cluster is experimentally computed with the value of 5.1 eV by Oku and coworkers.[35] This result is in agreement with the DFT calculation that is reported by Baei et al,.[36] The E_g values of $B_{12}N_{12}$ and $B_{16}N_{16}$ clusters are about 6.93 and 6.46 eV at the B3PW91 functional, respectively. With the adsorption of 5-AVA molecule at the B3PW91 method, the energy gaps of $B_{12}N_{12}$ and $B_{16}N_{16}$ clusters are significantly reduced to 5.14 and 5.68 eV, respectively. Whereas the energy gaps of 5-AVA molecule interacting with $B_{12}N_{12}$ and $B_{16}N_{16}$ clusters are decreased to 3.12 and 3.56 eV at the PBE method, respectively. We found that the calculations of E_g from both configurations in PBE method are close to the results of the theoretical data as mentioned above by Baei et al,.[36] The calculations of energy gap obtained by PBE and B3PW91 methods are significantly smaller than that of those obtained by B3LYP method.

Table 5 Calculated the structural and electronic properties of 5-aminolevulinic acid molecule interacted with $B_{12}N_{12}$ and $B_{16}N_{16}$ nano-cages at temperature 311.15 k.

	B3LYP		B3PW91		PBE	
System	$B_{12}N_{12}$	AVA/$B_{12}N_{12}$	$B_{12}N_{12}$	AVA/$B_{12}N_{12}$	$B_{12}N_{12}$	AVA/$B_{12}N_{12}$
$R_{B\text{-}N}$/ Å	1.487	1.565	1.485	1.565	1.494	1.573
$R_{B\text{-}N\text{-}B}$/°	80.50	83.81	80.12	83.80	79.94	83.45
$R_{N\text{-}B\text{-}N}$/°	98.23	92.09	98.44	92.15	98.58	92.53
D/Å	-	1.629	-	1.629	-	1.631
E_{ad}/eV	-	-1.18	-	-1.26	-	-1.34

Q_B /e	0.440	0.631	0.459	0.629	0.387	0.532
Q_N /e	-0.440	-0.517	-0.459	-0.517	-0.387	-0.456
$Q_{N\text{-}AVA}$ /e	-	-0.691	-	-0.696	-	-0.676
E_{HOMO}/eV	-7.71	-6.85	-7.89	-7.0	-6.78	-5.89
E_{LUMO} /eV	-0.87	-1.84	-0.90	-1.91	-1.72	-2.83
E_g/eV	6.84	5.01	6.99	5.09	5.06	3.06
ΔE_g (%)	-	-26.75	-	-27.18	-	-39.52
E_{FL}/eV	-4.29	-4.35	-4.40	-4.46	-4.25	-4.36
μ/eV	-4.29	-4.35	-4.40	-4.46	-4.25	-4.36
η/eV	3.42	2.51	3.50	2.55	2.53	1.53
ω/eV	2.69	3.77	2.76	3.90	3.57	6.21
S/eV	0.15	0.20	0.14	0.20	0.20	0.33
χ/eV	4.29	4.35	4.40	4.46	4.25	4.36
$D_{M/}$ Debye	0.00	7.89	0.00	7.57	0.00	7.58

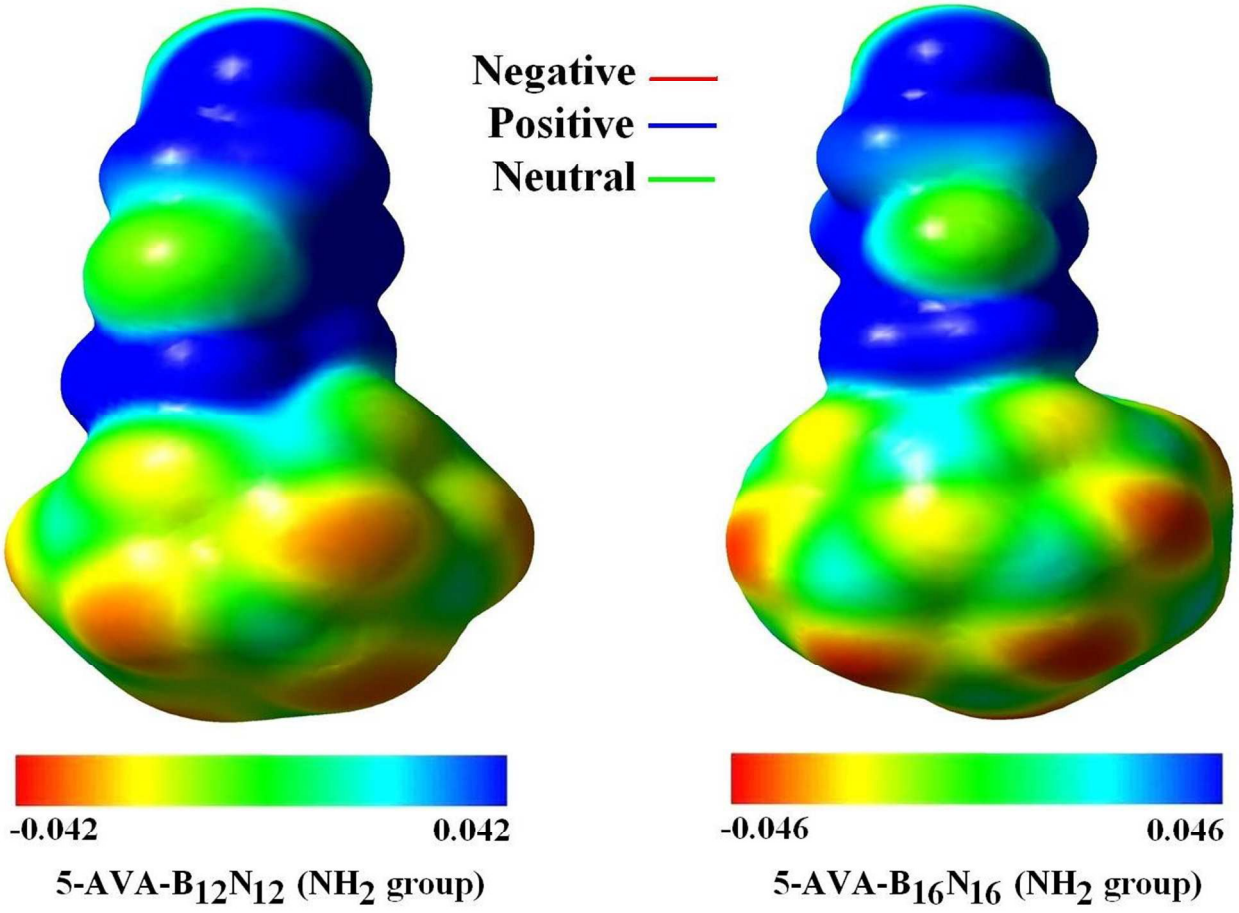

Fig. 5. The molecular electrostatic potential of 5-aminolevulinic acid molecule interacted with $B_{12}N_{12}$ and $B_{16}N_{16}$ nano-cages.

Table 6 Calculated the structural and electronic properties of 5-aminolevulinic acid molecule interacted with $B_{12}N_{12}$ and $B_{16}N_{16}$ nano-cages in solvent phase.

	B3LYP (H_2O)		B3PW91(H_2O)		PBE (H_2O)	
System	$B_{12}N_{12}$	AVA/$B_{12}N_{12}$	$B_{12}N_{12}$	AVA/$B_{12}N_{12}$	$B_{12}N_{12}$	AVA/$B_{12}N_{12}$
R_{B-N}/Å	1.486	1.578	1.484	1.574	1.494	1.583
R_{B-N-B}/°	80.54	83.96	80.11	83.62	79.95	83.63

$R_{N\text{-}B\text{-}N}$/°	98.18	91.24	98.46	91.60	98.60	91.64
D/Å	-	1.606	-	1.601	-	1607
E_{ad}/eV	-0.38	-1.42	-0.39	-1.51	-0.34	-1.59
Q_B/e	0.449	0.652	0.469	0.648	0.396	0.548
Q_N/e	-0.449	-0.509	-0.469	-0.522	-0.396	-0.447
$Q_{N\text{-}AVA}$/e	-	-0.705	-	-0.743	-	-0.685
E_{HOMO}/eV	-7.70	-6.96	-7.87	-7.12	-6.77	-6.02
E_{LUMO}/eV	-0.80	-1.07	-0.83	-1.13	-1.66	-2.11
E_g/eV	6.90	5.89	7.04	5.99	5.11	3.91
ΔE_g (%)	-	-14.64	-	-14.91	-	-23.48
E_{FL}/eV	-4.25	-4.02	-4.35	-4.13	-4.22	-4.07
μ/eV	-4.25	-4.02	-4.35	-4.13	-4.22	-4.07
η/eV	3.45	2.95	3.52	2.99	2.56	1.96
ω/eV	2.62	2.74	2.69	2.84	3.48	4.23
S/eV	0.14	0.17	0.14	0.17	0.19	0.26
χ/eV	4.25	4.02	4.35	4.13	4.22	4.07
$D_{M/}$ Debye	0.00	10.26	0.00	10.27	0.00	9.72

The quantum molecular descriptors (QMD) of reactivity in the context of DFT calculations are summarized in Table 2-5. When 5-AVA molecule (NH_2 group) is adsorbed on $B_{12}N_{12}$ nanocluster, the hardness values were reduced from 3.37, 3.47, and 2.50 eV in the pristine cluster to 2.49, 2.57, and 1.56 eV in the complexes at the B3LYP, B3PW91, and PBE methods, respectively, which means that the stability of the complexes are lower than pristine clusters.[37,38] The electrophilicity index of the drug molecule interacted with $B_{12}N_{12}$ cluster is drastically higher from 2.98, 2.94, and 3.91 eV in the pristine cluster to 3.80, 4.08, and 6.55 eV in the complexes at the B3LYP, B3PW91, and PBE methods, respectively, indicating higher

electrophilicity of a molecule which is greater than its electrophile character (see Tables 1, 2, and 3). TD-DFT calculation for 5-AVA drug molecule interacted with $B_{12}N_{12}$ nano-cluster was performed.[39] The details of these calculations are listed in Table 7. According to this Table 7, 5-AVA drug molecule has two excited states in wavelengths 400.01 and 394.01 nm with oscillator strengths (*f*) of 0.0015 and 0.0069 (at PBE method), respectively. The transition from HOMO-1 to LUMO is observed with 0.0069 of the oscillator strength and transition energy of 3.15 eV. There are two main transitions for the drug molecule at B3LYP method is observed in wavelengths of 278.26 and 275.06 nm with oscillator strengths of 0.0019 and 0.0049, respectively. In λ= 275.06 nm, electron is transferred from HOMO-1 to LUMO and mainly arising from $\pi \rightarrow \pi^*$ electronic excitations.[40,41] with 0.0049 of the oscillator strength and transition energy of 4.51 eV. The B3PW91 method contains two bands at 272.32 and 269.14 nm with having *f* values, 0.00298 and 0.0033, respectively. In wavelength of 269.14 nm, electron transfer occurred from HOMO-1 to LUMO, which has %66 that is the main transition. The UV–Vis absorption spectrum of 5-AVA drug molecule upon BN nanoclusters is shown in Fig. 6, with different basis sets. The UV–Vis absorption spectrum of PBE method exhibits a strong band at 394.01 nm. However, B3LYP method shows a band at 275.06 nm, and also the UV–Vis absorption spectrum of B3PW91 method exhibits a band at 269.14 nm. In Tables 2 and 3, the results show that the four highest and the four lowest molecular orbital energy levels of the 5-AVA drug molecule upon BN nanoclusters. Note that the HOMO–LUMO gap of the PBE method is relatively smaller than those of the other methods.

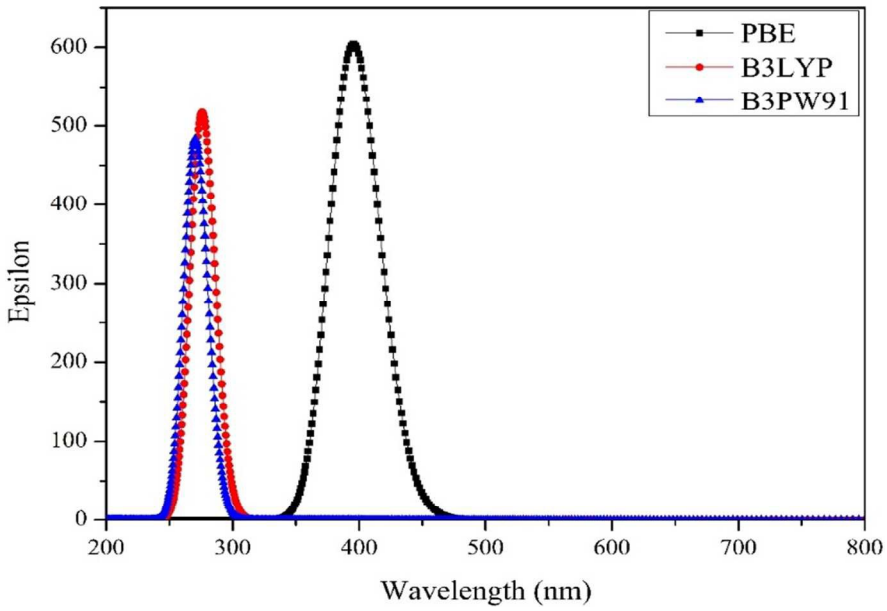

Fig. 6. UV-Vis Spectra of 5-aminolevulinic acid molecule (NH_2 group) upon $B_{12}N_{12}$ nano-cages.

The focus was made on photoinjection mechanisms from the excited electronic states of 5-AVA drug molecule with the $B_{12}N_{12}$ nano-cluster. Surface sensitization involves the adsorption of a 5-AVA drug molecule to the BN nanocluster surface and the formation of a 5-AVA-BN nanocluster surface compound. Photoexcitation of the surface compound can lead to interfacial electron transfer when there is a suitable energy match between the photoexcited electronic state in the surface compound and the electronic states in the HOMO-LUMO gap of the BN cluster. Injection times as short as a few femtoseconds have been investigated for various systems. According to Fig. 7, the time for electron injection in 5-AVA drug molecule is approximately 10 fs in $B_{12}N_{12}$ cluster. Fig. 8 shows the evolution of the time-dependent charge distribution during the early time relaxation dynamics after instantaneously populating the 5-AVA-LUMO, including the primary electron-transfer event within the first 2 fs of dynamics.

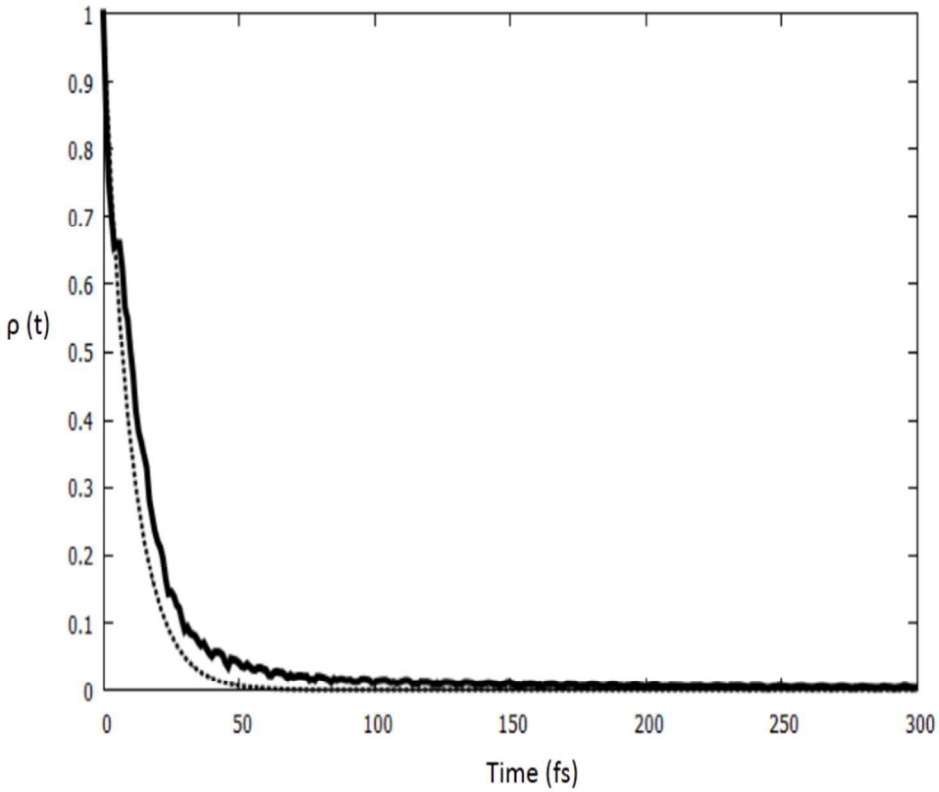

Fig. 7. Time-dependent survival probability in sensitized $B_{12}N_{12}$ nano-cage. The dashed lines are exponential fitting curves to the two elementary steps for electron transfer in the nano-cage.

Table 7 Selected excitation energies (eV, nm), oscillator strength (f), and relative orbital contributions of calculated at the most stable configuration.

Methods	Energy/eV	Wavelength/ nm	Oscillator Strength (*f*)	Assignment
B3LYP				
	4.55	278.26	0.0019	H → L (96%)
	4.51	275.06	0.0049	H-10 → L (12%), H-1 → L (82%)
B3PW91				H → L (91%), H-10 → L (4%)
	4.55	272.32	0.0029	H-10 → L (21%), H-1 → L (66%)
	4.61	269.14	0.0033	H-6 → L (3%), H → L (3%)
PBE				
	3.09	400.01	0.0015	H → L (99%)
	3.15	394.01	0.0069	H-1 → L (99%)

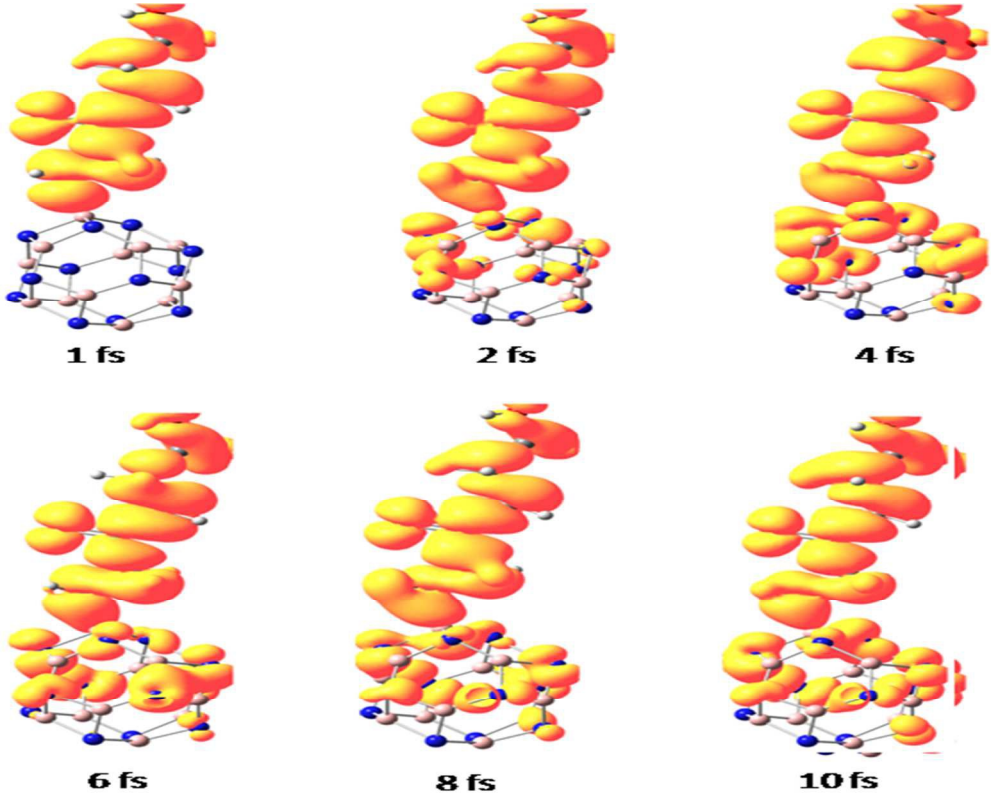

Fig. 8. Evolution of time-dependent charge distribution during the early time relaxation dynamics after instantaneously populating the 5-AVA drug molecule upon $B_{12}N_{12}$ nano-cage.

4. Concluding remarks

To conclude, we have investigated the binding and electronic properties of the covalent functionalization of $B_{12}N_{12}$ and $B_{16}N_{16}$ clusters with 5-aminolevulinic acid drug using DFT calculations. We found that the 5-AVA (NH_2 group) could be drug-loaded and covalently attached to $B_{12}N_{12}$ and $B_{16}N_{16}$ nanoclusters with almost similar binding energies of -2.01 and -1.95 eV at the B3LYP method, respectively, while the apparent results of the B3LYP method is fully different in comparison with B3PW91 and PBE methods. The functionalization of $B_{12}N_{12}$ and $B_{16}N_{16}$ clusters with 5-AVA drug indicate considerable influence in the electronic properties of adsorbent. NBO analysis predicts a significant charge transfer from drug molecule to adsorbents. We hope our results of the adsorption properties of 5-aminolevulinic acid upon the $B_{12}N_{12}$ and $B_{16}N_{16}$ nanoclusters can be used as an adsorbent enhancing delivery of drugs to cancer cells and decreasing drug interaction with healthy tissue.

Acknowledgments

We would like to thank the Nanotechnology Working Group of Young Researchers and Elite Club of Islamic Azad University, Gorgan Branch, Iran. We should thank the clinical Research Development Unit (CRDU), Sayad Shirazi Hospital, Golestan University of Medical Sciences, Gorgan, Iran.

References

1. S. Mukhopadhyay, R.H. Scheicher, R. Pandey, S. P. Karna, *J. Phys. Chem. Lett*. 2011, **2**, 2442.

2. S. Mukhopadhyay, S. Gowtham , R. H. Scheicher, R. Pandey, S. P. Karna, *Nanotechnology,* 2010, **21,** 165703.

3. C.Y. Zhi, Y. Bando, C. C. Tang, R. Xie, T. Sekiguchi, D. Golberg, *J. Am. Chem. Soc*, 2005, **127**, 15996.

4. C. Y. Zhi, Y. Bando, C. C. Tang, D. Golberg, *Phys. Rev. B,* 2006, **74**, 153413.

5. C. Y. Zhi, Y. Bando, C.C. Tang, Q. Huang, D. Golberg, *J. Mater. Chem*, 2008, **18**, 3900.

6. D. Golberg, Y. Bando, C. C. Tang, C. Y. Zhi, *Adv. Mater*, 2007, **19**, 2413.

7. A. Soltani, N. Ahmadian, Y. Kanani, A. Dehno khalaji, H. Mighani, *Appli. Surf. Sci*, 2012, **258**, 9536.

8. A. Soltani, N. Ahmadian, A. Amirazami, A. Masoodi, E. Tazikeh Lemeski, Ali Varasteh Moradi, *Appli. Surf. Sci,* 2012, **261**, 262.

9. W. L. Wang, Y. Bando, C. Y. Zhi, W. F. Fu, E. G. Wang, D. Golberg, *J. Am. Chem. Soc*, 2008, **130**, 8144.

10. G. Ciofani, V. Raffa, A. Mencissi, P. Dario, *J. Nanosci. Nanotech*, 2008, **8**, 6223.

11. C. Y. Zhi, J. L. Zhang, Y. Bando, T. Terao, C. C. Tang, H. Kuwahara, D. Golberg, *J. Phys. Chem. C*, 2008, **112**, 17592.

12. G. Ciofani, V. Raffa, A. J. Yu, Y. Chen, Y. Obata, S. Takeoka, A. Mencissi, A. Cuschieri, *Current Nanosci*, 2009, **5**, 33.

13. M. Mirzaei, *Superlattic. Microstructur*, 2013, **57**, 44.

14. E. Erdtman, L. A. Eriksson, *Chem. Phys. Lett*, 2007, **434**, 101.

15. T. Patrice (Ed.), Photodynamic Therapy, RSC Publishing, 2004.

16. R. Baumgartner, R. Pottier, B. Krammer, H. Stepp (Eds.), Photodynamic Therapy with ALA, RSC Publishing, 2006, and references therein.

17. Q. Peng, T. Warloe, K. Berg, J. Moan, M. Kongshaug, K.-E. Giercksky, J. M. Nesland, *Cancer*, 1997, **79**, 2282.

18. M. D. Ganji, H. Yazdani, A. Mirnejad, *Physica E*, 2010, **42**, 2184.

19. G. Gou, B. Pan, L. Shi, *ACS Nano*, 2010, **4**, 1313.

20. S. Y. Xie, W. Wang, K. A. S. Fernando, X. Wang, Y. Lin, Y. P. Sun, *Chem. Commun*, 2005, **29**, 3670.

21. J-X. Zhao, Y-h. Ding, *Diamond & Related Materials*, 2010, **19**, 1073.

22. C. Y. Zhi, Y. Bando,W. L. Wang, C. C. Tang, H. Kuwahara, D. Golberg, *Chem. Asian J*, 2007, **2**, 1581.

23. M. Kia, M. Golzar, K. Mahjoub, A. Soltani, *Superlattic. Microstructur*, 2013, **62**, 251.

24. M. W. Schmidt, K. K. Baldridge, J. A. Boatz, S. T. Elbert, M. S. Gordon, J. H. Jensen, S. Koseki, N. Matsunaga, et al, *J. Comput. Chem*, 1993, **14**, 1347.

25. A. Ahmadi Peyghan, N. Hadipour, Z. Bagheri, *J. Phys. Chem. C*, 2013, **117**, 2427.

26. J. Beheshtian, A. Ahmadi Peyghan, M. Noei, *Sensors and Actuators B*, 2013, **181**, 829.

27. S. F. Rastegar, A. Ahmadi Peyghan, N. L. Hadipour, *Appli. Surf. Sci*, 2013, **265**, 412.

28. A. Bahrami, S. Yourdkhani, M. D. Esrafili, N. L. Hadipour, *Sensors and Actuators B*, 2014, **191**, 457.

29. J. P. Perdew, K. Burke, M. Ernzerhof, *Phys. Rev. Lett*, 1996, **77**, 3865.

30. A. D. J. Becke, *J. Chem. Phys*, 1993, **98**, 5648.

31. R.G. Pearson, *Proc. Nati. Acad. Sci.*, 1986, **83**, 8440.

31. A. Soltani, M. T. Baei, A. S. Ghasemi, E. Tazikeh Lemeski, K. Hosseni Amirabadi, *Superlattices and Microstructures*, 2014, **75**, 564.

32. A. Soltani, M. T. Baei, E. Tazikeh Lemeski, A. A. Pahlevani, *Superlattic. Microstructur*, 2014, **75**, 716.

33. E. C. Anota, G. H. Cocoletzi, *Physica E*, 2014, **56**, 134.

34. N. Saikia, S. K. Pati, R. C. Deka, *Appl. Nanosci*, 2012, **2**, 389.

35. T. Oku, A. Nishiwaki, I. Narita, Sci. Technol. *Adv. Mater*. 2004, **5**, 635.

36. M. T. Bae, *Comput. Theor. Chem*, 2013, **1024**, 28.

37. N. Saikia, R. C. Deka, *Comput. Theor. Chem*, 2011, **964**, 257.

38. Z. B. Nojini, F. Yavari, S. Bagherifar, *J. Mole. Liquids*, 2012, **166**, 53.

39. H. Ullah, A-u-H. Ali Shah, S. Bilal, K. Ayub, *J. Phys. Chem. C*, 2013, **117**, 23701.

40. N. Sanna, G. Chillemi, L. Gontrani, A. Grandi, G. Mancini, S. Castelli, G. Zagotto, C. Zazza, V. Barone, A. Desideri, *J. Phys. Chem. B*, 2009, **113**, 5369.

41. A. Soltani, M. Bezi Javan, *RSC Adv*., 2015, **5**, 90621.

Table of Contents:

5-aminolevulinic acid-functionalized $B_{12}N_{12}$ and $B_{16}N_{16}$ nanoclusters were studied, showing significant UV-Vis adsorption spectrum at 200 to 300 nm.

Image